Biomedical Physics & Engineering Express

Endorsed by IPEM Institute of Physics and Engineering in Medicine

PAPER • **OPEN ACCESS**

The use of dynamic CT imaging for tracking mandibular movements in a phantom

To cite this article: Stijn E F Huys *et al* 2023 *Biomed. Phys. Eng. Express* **9** 015002

Biomedical Physics & Engineering Express

PAPER

The use of dynamic CT imaging for tracking mandibular movements in a phantom

Stijn E F Huys[1,2,4], **Benyameen Keelson**[3,4], **Yannick de Brucker**[3], **Gert Van Gompel**[3], **Johan de Mey**[3], **Jos Vander Sloten**[1] **and Nico Buls**[3,*]

[1] Engineering Science, section of Biomechanics, Catholic University of Leuven, Leuven, Belgium
[2] CADskills BV, Ghent, Belgium
[3] Department of Radiology, Universitair Ziekenhuis Brussel (UZ Brussel), Vrije Universiteit Brussel (VUB), Laarbeeklaan 101, 1090 Brussels, Belgium
[4] Co-first authors who contributed equally.
[*] Author to whom any correspondence should be addressed.

E-mail: Nico.Buls@uzbrussel.be

Keywords: temporomandibular joint, four-dimensional computed tomography, radiometry, mandible, phantoms, imaging

OPEN ACCESS

RECEIVED
10 June 2022

REVISED
5 October 2022

ACCEPTED FOR PUBLICATION
16 November 2022

PUBLISHED
25 November 2022

Abstract

Purpose. The objective of this study was to analyse the possibilities of using 4D CT scanning for the tracking of patients' mandibles. *Methods*. A clinical 256-slice Revolution CT was used in obtaining 4D CT scans without table movement, with a novel mandibular phantom, mounted on a programmable six degrees-of-freedom Stewart Platform in motion. The phantom was used to simulate mandibular motions which are combinations of rotations with translations (depression, elevation, protrusion, retrusion and laterotrusion). The phantom was scanned five times during identical motion patterns with a dynamic CT acquisition protocol. An image processing workflow consisting of a pairwise rigid registration and semi-automatic segmentation was developed to extract kinematic parameters (cardan angles and point-of-interest displacements) from the dynamic sequences. Reproducibility was investigated by the 95% confidence interval and the absorbed organ dose to organs of interest in the primary beam were also estimated and compared to those of a standard CT scan of the brain *Results*. The maximum average 95% confidence interval for the displacement across all time points for the five repetitions was 0.61 mm (*Y* axis). In terms of rotations, the maximum average 95% confidence interval across all time points for the five repetitions was 1.39° (*X* axis). The effective dose for the dynamic scan was found to be 1.3 mSv, for a $CTDI_{vol}$ of 63.95 mGy and a DLP of 1023.14 mGycm. The absorbed organ doses were similar to organ doses during a clinical head CT scan. *Conclusions*. A framework is proposed to use 4D CT scanning as a possible methodology to evaluate the motion of the temporomandibular joint. The scanning protocol allows to visualise the motion by applying a semi-automated segmentation and registration. A graphical representation of all displacements in the three spatial dimensions can depict multiple points-of-interest at once during the same acquisition. A novel type of phantom was also introduced which simulates mandibular movement with six degrees-of-freedom (three translations and three rotations).

Introduction

The temporomandibular joints (TMJs) are very complex and unique joints [1] in the human body: both sides are connected to each other by the mandible, and it is the only joint in the human body that allows for a hinge and slide (rotation and translation) motion during its operation. Non- or minimally invasive surgery can be applied to most of the temporomandibular disorders (TMD), but when tissue-sparing surgery is not an option anymore, a total temporomandibular joint prosthesis is often the only remaining option. After surgery, patients that have undergone such a joint replacement usually have limited movement capabilities. Research by De Meurechy *et al* has shown that post-operative physiotherapy plays an important role in achieving good postoperative results [2].

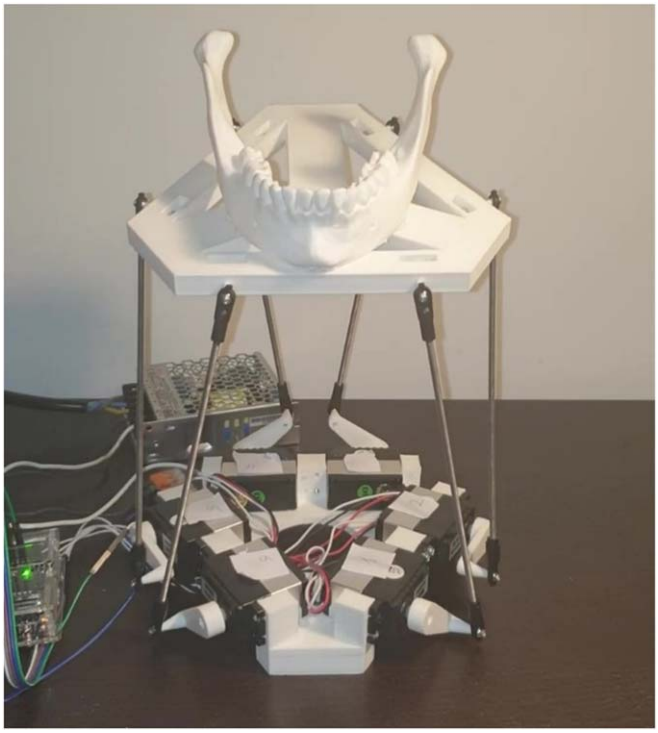

Figure 1. Dynamic six degrees-of-freedom phantom of the mandible.

Even though various methods are described for the evaluation of occlusion and mandibular movement registration, limited methodologies exist to monitor the functionality of the (diseased) temporomandibular joints, especially the dynamic behaviour. Besides methods like simply calculating certain condylar positions by measuring and converting mandibular excursions or the use of a kinematic facebow, there are also evaluation methods reported using x-ray imaging, e.g.: single-plane fluoroscopy [3, 4], CBCT (cone-beam CT) [3], and conventional computed tomography (3D CT) [5]. They have inherent drawbacks, ranging from providing only limited information (absence of motion information due to only static images; only 2D information) to methodologies that are difficult to implement in a daily clinical workflow. A detailed analysis of condylar behaviour during movement can be of potential interest to evaluate the progress of the revalidation of the patient. This might be fulfilled by dynamic 4D CT scanning, which adds a time dimension to 3D images.

The clinical use of 4D CT scanning has seen a vast increase in the last two decades, with investigation and visualization opportunities ranging from cardiac [6, 7] and lung [8] applications and from research in the central nervous system [7, 9, 10, 11] to dynamic MSK applications in several joints (lower limb [12], wrist [13, 14, 15]) and many other fields [16]. In addition to providing 3D morphological information, this method allows clinicians and radiologists to evaluate multiple timeframes and thus the motion of the inspected structures.

A case study by Akashi *et al* showed promising results in using 4D CT for the evaluation of jaw movement following mandibular reconstruction [17], but no further research was done on this subject, especially regarding optimization and validation of the protocol, in particular for rehabilitation purposes.

Until now, a few static or rotary phantoms were used in the validation of 4D CT scanning [18], but such technical phantoms do not represent the anatomical complexity and motion of a mandible. A six degrees-of-freedom (DOF) phantom is more suited to evaluate the complex combinations of rotations and translations of the TMJ.

The goal of this experimental phantom study was to evaluate the feasibility of using dynamic CT scans to track the progress of rehabilitating TMJ patients by recording the motion of this joint. This was done by establishing a scanning protocol and a realistic mock-up phantom with detailed anatomical representation. In addition, the complete image processing workflow was set in place and the radiation dose to the patient was simulated using a humanoid virtual phantom.

Materials and methods

To simulate mandibular movements with variable speeds a 3D printed phantom was developed based on segmented DICOM CT data of a healthy male jaw (excluding temporal bone, retrieved from a head CT from the radiology database) using Mimics Innovation Suite 23, Materialise, Heverlee, Belgium) (figure 1). The phantom is based on the Stewart Platform

Figure 2. The clinical 256-slice Revolution CT (GE Healthcare, Waukesha, Wisconsin, USA) (left) which was used to obtain continuous scans without table movement while the phantom (right) was in motion.

principle [19], which is a parallel manipulator with six degrees-of-freedom (DOF) (forward/back, up/down, left/right, yaw, pitch, roll) and which is often used in flight simulators, robotics and additive manufacturing. The device consists of a base plate which contains six servo motors (Reely Standard Analog Servo RS-606WP MG, 55 Ncm, 4,8–6 V) that transform their rotary motion into translations and rotations of the upper plate via M3 rods and M3 ball heads. The motors are driven by a microcontroller (Joy-IT UNO R3 DIP with an ATMega328 microcontroller, Arduino compatible) and a separate adjustable switching power supply (Mean Well LRS-50-5, 10 A, 50 W, 5 V/DC), using different scripts (C/C++) in the Arduino IDE (Arduino Software, Interaction Design Institute, Ivrea, Italy) for simulating the five different motions of the mandible [20]: depression, elevation, protrusion, retrusion and laterotrusion. Both the upper and lower platforms and the phantom mandible are manufactured by fused filament fabrication of polylactic acid (PLA) using an Ultimaker 3 (Ultimaker BV, Geldermalsen, The Netherlands) printer. To avoid scattering and interference of the motors with the scanner, the platform is mounted sideways, so that only the PLA mandible is in the scanner field-of-view.

A clinical 256-slice Apex Revolution CT (GE Healthcare, Waukesha, Wisconsin, USA) was used in obtaining continuous volume scans without table movement while the phantom was in motion (figure 2). The Dose Length Product (DLP) and Computer Tomography Dose Index ($CTDI_{vol}$) were recorded and the potential organ and effective doses were calculated by the voxel based dosimetry model of the National Cancer Institute [21]. Table 1 shows details of the scan parameters. In addition, the dose of a standard CT scan of the brain (DLP = 1000 mGy, $CTDI_{vol}$ = 60 mGy) was considered for comparison [22]. Figure 3 illustrates the scan range used for organ dose and effective dose estimations for the dynamic scan of the jaw and that of a clinical brain scan.

Table 1. Details of the scan parameters used during the studied scanning protocol.

Scan parameter	Value
Tube voltage	120 kV
Tube current	80 mA
Tube rotation time	0.28 s
Reconstructed slice thickness	1.25 mm
Reconstructed Field of View	320 mm
Collimation	128 × 1.25 mm
Dose length product	1023 mGycm
CTDI	63.9 mGy
ASIR-level	50%
Image matrix	512 × 512
Scan duration	6 s

Motion information was obtained by a voxel-based pairwise rigid registration between the image data from each time point in the dynamic scan sequence with a reference image chosen from within the sequence. The pairwise rigid registration can be mathematically expressed as

$$\hat{\mu} = argmin\ C(f(\boldsymbol{x}), g_n(T_\mu(\boldsymbol{x}))), \quad (1)$$

where f represents the reference image (chosen by the user), g_n represents one of the subsequent images

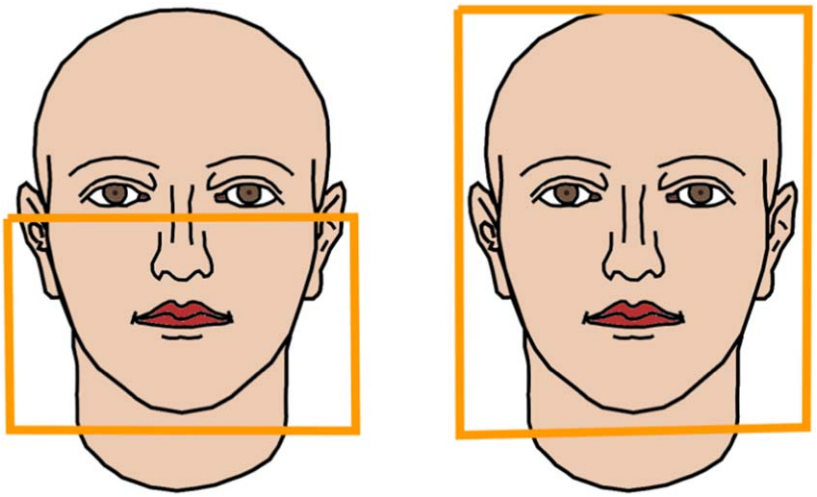

Figure 3. The scan range used for organ dose and effective dose estimations for a dynamic scan of the jaw (left) and that of a clinical brain scan (right).

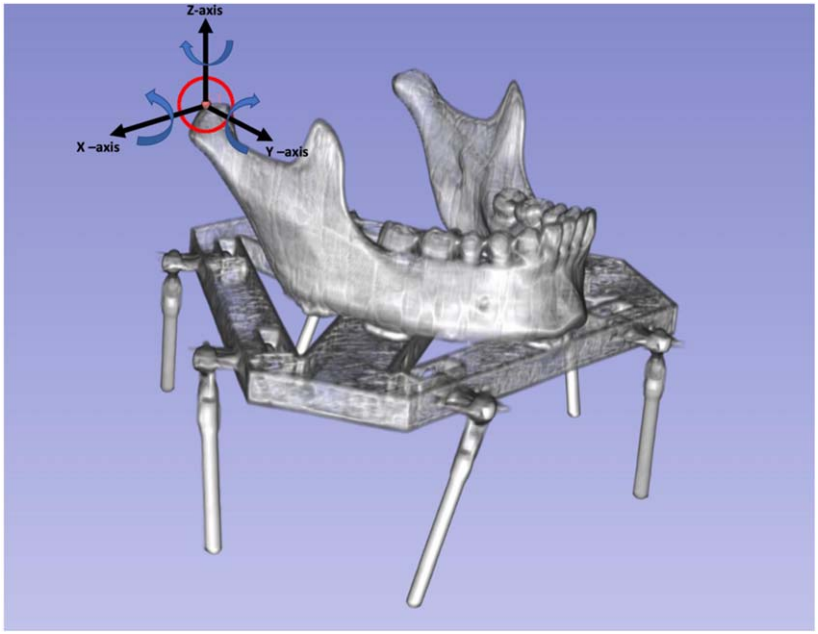

Figure 4. The segmented mandible on top of the phantom Stewart Platform. Point-of-interest F-1 is indicated with a circle. The three axes describing the directions of displacement of the point (black arrows) and the rotations around these axes (grey arrows) are also shown. The described axes follow the reference frame of the CT, where X represents the left-right axis, Y represents the anterior-posterior axis and Z represents the inferior-superior axis.

depicting the phantom in the various phases of motion and x is a vector of the spatial coordinates over the image. The transformation T which aligns the two images was optimized over a set of parameters μ. The quality of alignment between the reference image and the dynamic time points is determined by the cost function C (similarity metric). The segmented reference image facilitated the computation of the cost function over the temporomandibular joint and its immediate vicinity.

A series of rigid transformation matrices (T,t) were estimated for each time point (t). Cardan angles were extracted to describe the motion of the phantom. In addition, the displacement of a point-of-interest (POI) manually placed on the right mandibular condyle of the static image (figure 4) was computed by transforming the point using the obtained transformation matrices.

The most common mandibular extrusions were combined in one single motion sequence which was then scanned and analysed. The movement contained the following specific order in 4.5 seconds (which was continuously repeated): a mandibular depression, protrusion, laterotrusion to the left, laterotrusion to the right, retrusion and mandibular elevation. The

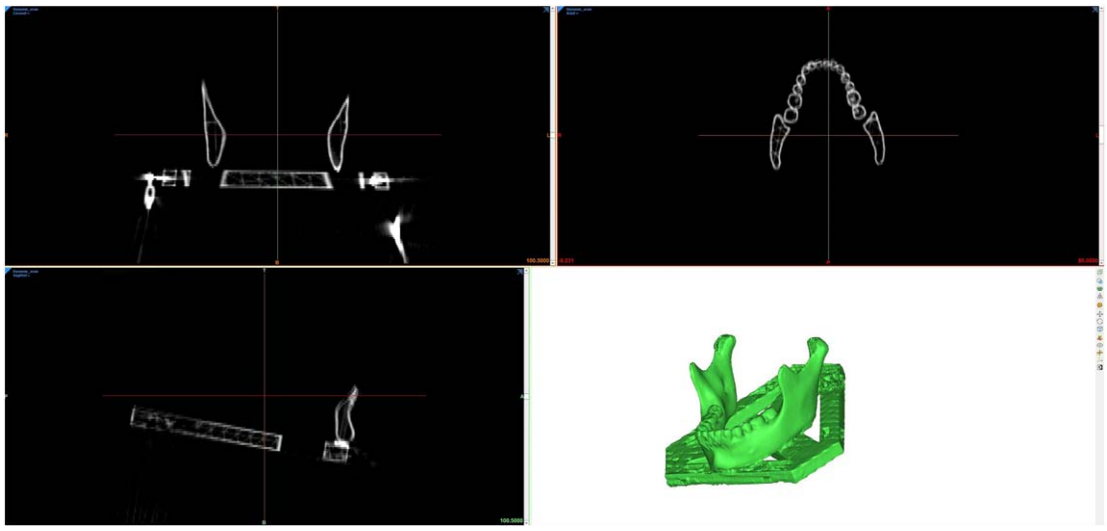

Figure 5. A coronal (upper row, left), axial (upper row, right) and sagittal (bottom row, left) static image and volume rendered image (bottom row, right) of the mandible phantom.

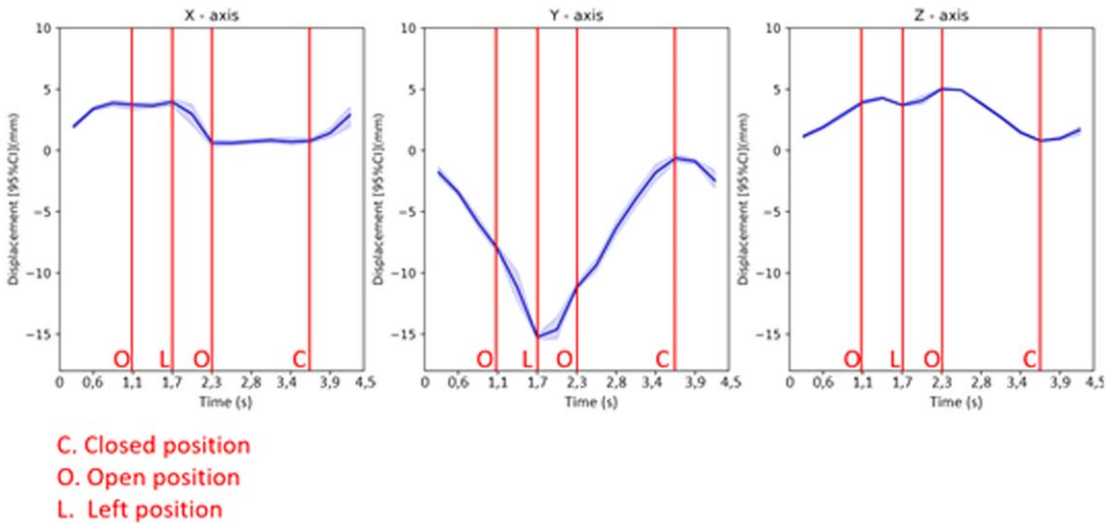

Figure 6. The tracking of point-of-interest F-1 in all three main directions of the scanner during the combined motion of the phantom. Shaded regions represent the 95% confidence interval for the five repetitions.

(maximum) excursions of the phantom jaw motion are based on measurements done by hand according to the clinical protocol used in the craniomaxillofacial surgery department: using a jaw scale (TheraBite Range of Motion Scale), the maximal positions of the jaw during depression, left/right laterotrusion and protrusion are measured and programmed into the phantom. The magnitudes of these motions were derived from mandibular excursions on a healthy subject, which are typically larger and faster than those of a TMJ patient [23]. The phantom's movement was scanned five times (without temporal synchronization) and the 95% confidence interval across all time points for the five repetitions was evaluated as a measure of reproducibility. This confidence interval was determined based on the tracked displacement (in the three main directions of the scanner) of the POI and the cardan angles of the phantom.

Results

Figure 5 shows CT images of the phantom and a volume rendered image. Figure 6 shows that the predominant displacement can be observed along the *Y*-axis (of the scanner) which agrees with the motion of the phantom during the CT acquisition. Cardan angles describing rotations around the three axes for the entire jaw phantom are shown in figure 7. The predominant rotation is observed around the *X*-axis with minimal rotation around the *Z*- and *Y*-axes. The average 95% confidence interval for the displacement across all time points for the five repetitions was

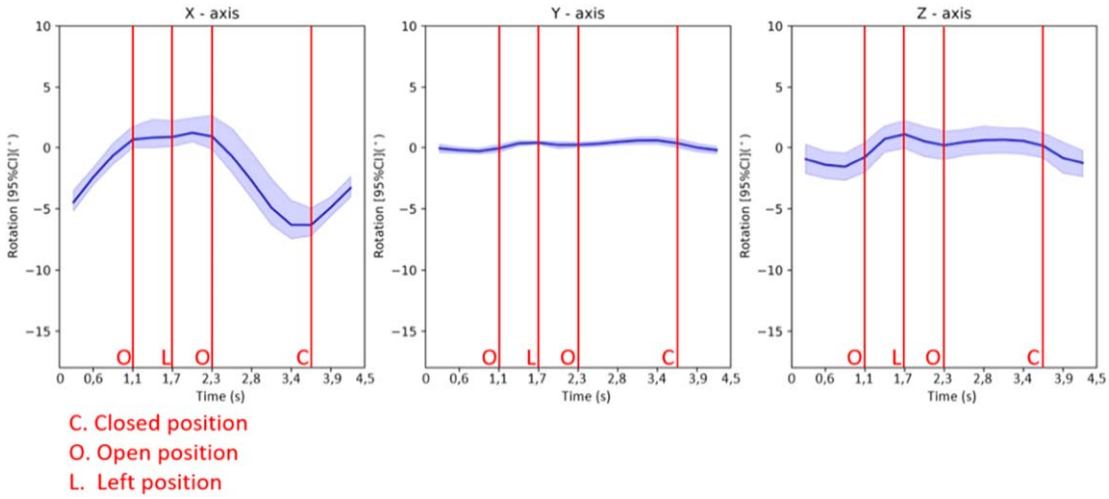

Figure 7. Cardan angles in all three main directions of the scanner during the combined motion of the phantom. Shaded regions represent the 95% confidence interval for the five repetitions.

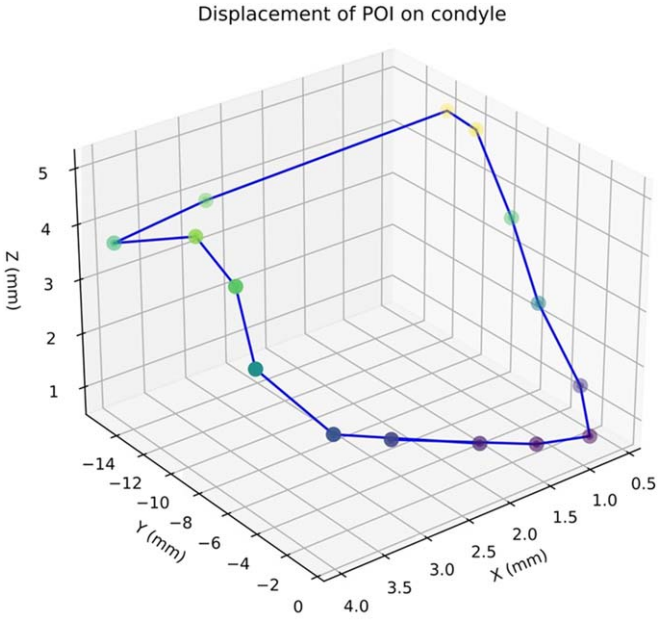

Figure 8. 3D plot representing the displacement of the POI. The different colorscales represent different time frames.

0.41 mm (relative variation: 9.1%), 0.61 mm (relative variation: 3.9%) and 0.20 mm (relative variation: 4.0%) for the *X*-, *Y*- and *Z*- axis respectively. In terms of rotations, average 95% confidence interval across all time points for the five repetitions were 1.39° (relative variation: 21.4%), 0.31° (relative variation: 62.0%) and 1.29° (relative variation: 64.5%) for the *X*-, *Y*- and *Z*-axis respectively. Figure 8 shows a 3D plot representing the displacement of the POI.

The effective dose for the dynamic scan was found to be 1.3 mSv, for a $CTDI_{vol}$ of 63.9 mGy and a DLP of 1023 mGycm. Doses to organs of interest are presented in table 2, including a comparison to doses for a clinical head CT scan.

Discussion

Our study showed that quantitative information of TMJ movement can be obtained from a single dynamic CT scan. The phantom with six degrees-of-freedom is adaptable for multiple cases: the combination of a translation in all three directions (X, Y and Z) and all rotations (pitch, jaw and roll) allows researchers to create biomimetic movements, similar to those of healthy subjects (whose excursions are faster and larger than those of people with diseased TMJs [23]).

The rigid registration of the dynamic CT images facilitated the computation of transformation matrices from which 6 DOF kinematic motion parameters

Table 2. Comparison between the organ doses in this study and those in a clinical brain scan according to European diagnostic reference levels.

Organ	Organ dose for a dynamic CT scan of the mandible (mGy) (Effective dose: 1.3 mSv)	Organ dose for a clinical brain scan (mGy) (Effective dose: 1.5 mSv)
Brain	10.8	43.0
Salivary glands	49.0	40.3
Pituitary gland	36.6	41.5
Eye lens	27.4	49.5
Oral cavity	36.6	33.8
Spinal cord	8.6	6.3
Thyroid	2.9	1.8

were extracted. The workflow resulted in reproducible kinematic parameters across all axes (average 95% confidence interval below 0.6 mm and 1.4°), as is shown from the five repeated experiments.

Dose to the patient is of importance in any imaging modality that involves ionizing radiation. The effective dose for the dynamic scan was 1.3 mSv, comparable to that of a routine clinical adult brain CT scan (1.5 mSv [24, 25]), but higher than that of a CBCT (0.1–0.35 mSv [26]). Since the temporomandibular joints are located rather close to the eyes, the dose reaching the eye and other organs in this region is of concern. The absorbed dose to the eye lens in this dynamic study was 27.4 mGy which lies below the reported range of 30–50 mGy associated with CT scanning of the head [27]. The positions of the patient's head can also be further optimized to reduce this dose. The head can be tilted backwards to prevent direct radiation passing through the eyes, but this can influence the measured motions, since this tensions muscles needed for the movements and prevents a full range-of-motion of the mandible.

Visual and graphical motion representation of all mandibular extrusions potentially provide craniomaxillofacial surgeons valuable information for postoperative evaluation and follow-up of patients that potentially suffer from temporomandibular joint disorders. Such information could potentially contribute to optimise the patients' treatment and rehabilitation plan. The graphical 3D representation of the displacements in all directions of certain points-of-interest can be an addition to the Range Of Motion measurement in the Helkimo Index (an index to assess temporomandibular disorders in a specified population) [28], which is currently measured by hand in only two dimensions. Especially since multiple points-of-interests can be evaluated during the exact same motion (and thus, no inter-cycle variability is present), e.g., both condyles and the incisor teeth. These measurements could now be (semi-)automated to allow the surgeon to investigate these excursions in 3D rather than a simplified frontal measurement. This methodology can then even be considered to reconstruct a patient-specific Posselt's envelope of motion [20] in 3D, both before surgery and during rehabilitation, which potentially offers useful information to the surgeon. An additional advantage of this technique is the fact that the images can be used further in the process, during for example the design of patient specific total temporomandibular joint replacement implants

A limitation to this study is the lack of a validation of the motion kinematics estimated from the dynamic images. The use of a Vicon set-up (3D motion capture system) or a Kinect system (motion sensing input devices produced by Microsoft) could provide kinematics parameters which can be compared to the motion parameters obtained by dynamic CT. Secondly, we did not consider the effect of metal artifacts caused by the potential presence of implants. Thirdly, different motion ranges and speeds were not evaluated. Lastly, this research was performed on a polymer mandible, without representative soft and hard (temporal bone) tissue materials. However, research by Keelson *et al* [29] has shown that this scanning and registration protocol is also applicable in human subjects (who have both soft and hard tissues). Further validation (e.g. via clinical trials) should still be carried out, before applying this protocol to patients.

Conclusion

A framework is proposed to use 4D CT scanning as a potential methodology to evaluate the motion of the temporomandibular joint. The scanning protocol allows to visualise the motion by applying a semi-automated segmentation and registration. A graphical representation of all displacements in the three spatial dimensions can depict multiple points-of-interest at once during the same acquisition. A novel type of phantom was also introduced which simulates mandibular movement with six degrees-of-freedom (three translations and three rotations).

Acknowledgments

This research was funded by the Baekeland scheme of the Flanders Agency for Innovation and Entrepreneurship (VLAIO), HBC.2017.0575.

Data availability statement

The data that support the findings of this study are available upon reasonable request from the authors.

ORCID iDs

Stijn E F Huys https://orcid.org/0000-0002-6121-901X

References

[1] Saad A, Winters R, Wise M W, Dupin C L and St.hilaire H 2013 Virtual surgical planning in complex composite maxillofacial reconstruction *Plast Reconstr Surg* **132** 626–33

[2] De Meurechy N K G, Loos P J and Mommaerts M Y 2019 Postoperative physiotherapy after open temporomandibular joint surgery: A 3-step program *J. Oral Maxillof. Surg.* **77** 932–50

[3] Chen cc, Lin cc, Chen Y J, Hong S W and Lu T W 2013 A method for measuring three-dimensional mandibular kinematics *in vivo* using single-plane fluoroscopy *Dentomaxillofacial Radiology* **42** 95958184

[4] Taniguchi H, Matsuo K, Okazaki H, Yoda M, Inokuchi H, Gonzalez-Fernandez M, Inoue M and Palmer J B 2013 Fluoroscopic evaluation of tongue and jaw movements during mastication in healthy humans *Dysphagia* **28** 419–27

[5] Terajima M, Endo M, Aoki Y, Yuuda K, Hayasaki H, Goto T K, Tokumori K and Nakasima A 2008 Four-dimensional analysis of stomatognathic function *American Journal of Orthodontics and Dentofacial Orthopedics* **134** 276–87

[6] Peyrat J M, Delingette H, Sermesant M, Xu C and Ayache N 2010 Registration of 4D cardiac CT sequences under trajectory constraints with multichannel diffeomorphic demons *IEEE Trans. Med. Imaging* **29** 1351–68

[7] Kuroda J, Kinoshita M, Tanaka H, Nishida T, Nakamura H, Watanabe Y, Tomiyama N, Fujinaka T and Yoshimine T 2012 Cardiac cycle-related volume change in unruptured cerebral aneurysms: A detailed volume quantification study using 4-dimensional ct angiography *Stroke* **43** 61–6

[8] Albert J, Labarbe R, Janssens G, Souris K and Sterpin E 2019 Estimation of respiratory phases during proton radiotherapy from a 4D-CT and Prompt gamma detection profiles *Physica Med.* **64** 33–9

[9] Siebert E, Diekmann S, Masuhr F, Bauknecht H C, Schreiber S, Klingebiel R and Bohner G 2012 Measurement of cerebral circulation times using dynamic whole-brain CT-angiography: Feasibility and initial experience *Neurological Sciences* **33** 741–7

[10] Suzuki K, Morita S, Masukawa A, Machida H and Ueno E 2010 Diagnosing a large slowly enhanced cerebral aneurysm using four-dimensional multiphase dynamic contrast-enhanced computed tomography angiography *Jpn J Radiol* **28** 680–3

[11] Willems P W A, Taeshineetanakul P, Schenk B, Brouwer P A, Terbrugge K G and Krings T 2012 The use of 4D-CTA in the diagnostic work-up of brain arteriovenous malformations *Neuroradiology* **54** 123

[12] Buzzatti L, Keelson B, Vanlauwe J, Buls N, De Mey J, Vandemeulebroucke J, Cattrysse E and Scheerlinck T 2021 Evaluating lower limb kinematics and pathology with dynamic CT *Bone Joint J* **103-B** 822–7

[13] Leng S, Zhao K, Qu M, An K N, Berger R and McCollough C H 2011 Dynamic CT technique for assessment of wrist joint instabilities *Med. Phys.* **38** S50–6

[14] Choi Y S, Lee Y H, Kim S, Cho H W, Song H T and Suh J S 2013 Four-dimensional real-time cine images of wrist joint kinematics using dual source CT with minimal time increment scanning *Yonsei Med J* **54** 1026–32

[15] Troupis J M and Amis B 2013 Four-dimensional computed tomography and trigger lunate syndrome *J. Comput. Assist. Tomogr.* **37** 639–43

[16] Kwong Y, Mel A O, Wheeler G and Troupis J M 2015 Four-dimensional computed tomography (4DCT): a review of the current status and applications *J Med Imaging Radiat Oncol* **59** 545–54

[17] Akashi M, Shibuya Y, Takahashi S, Hashikawa K, Hasegawa T, Kakei Y, Negi N, Sekitani T and Komori T 2016 Four-dimensional computed tomography evaluation of jaw movement following mandibular reconstruction: a pilot study *J. Cranio Maxillof. Surg.* **44** 637–41

[18] Keelson B, Buzzatti L, Lopez V P, Scheerlink T, Gompel G V, Cattrysse E, Mey J de, Vandemeulebroucke J and Buls N 2020 Quantifying motion artifacts using a rotating phantom: insights towards dynamic musculoskeletal applications *Medical Imaging 2020: Physics of Medical Imaging* **11312** 1131230

[19] Dasgupta B and Mruthyunjaya T S 2000 The Stewart platform manipulator: a review *Mech. Mach. Theory* **35** 15–40

[20] Posselt U and Andersen A 1952 *Studies in the mobility of the human mandible* (Acta Odontologica Scandinavica) 160

[21] Lee C, Kim K P, Bolch W E, Moroz B E and Folio L 2015 NCICT: a computational solution to estimate organ doses for pediatric and adult patients undergoing CT scans *J. Radiol. Prot.* **35** 891

[22] Anon 2014 Radiation protection N° 180: diagnostic reference levels in thirty-six european countries *European Commission*

[23] Sinn D P, De Assis E A and Throckmorton G S 1996 Mandibular excursions and maximum bite forces in patients with temporomandibular joint disorders *J Oral Maxillofac Surg* **54** 671–9

[24] McCollough C H, Bushberg J T, Fletcher J G and Eckel L J 2015 Answers to common questions about the use and safety of CT scans *Mayo Clin Proc* **90** 1380–92

[25] Mettler F A *et al* 2020 Patient exposure from radiologic and nuclear medicine procedures in the United States: Procedure volume and effective dose for the period 2006–2016 *Radiology* **295** 418–27

[26] Daly M J, Siewerdsen J H, Moseley D J, Jaffray D A and Irish J C 2006 Intraoperative cone-beam CT for guidance of head and neck surgery: assessment of dose and image quality using a C-arm prototype *Med. Phys.* **33** 3767–80

[27] Lee Y H, Yang S H, Lin Y K, Glickman R D, Chen C Y and Chan W P 2020 Eye shielding during head CT scans: dose reduction and image quality evaluation *Acad. Radiol.* **27** 1523–30

[28] Helkimo M 1974 Studies on function and dysfunction of the masticatory system. II. Index for anamnestic and clinical dysfunction and occlusal state *Sven Tandlak Tidskr* **67** 101–21

[29] Keelson B *et al* 2021 Automated motion analysis of bony joint structures from dynamic computer tomography images: A multi-atlas approach *Diagnostics* **11** 2062